

Octahedral Non-helical Bis(bipyridyl) Metallomacrocycles†

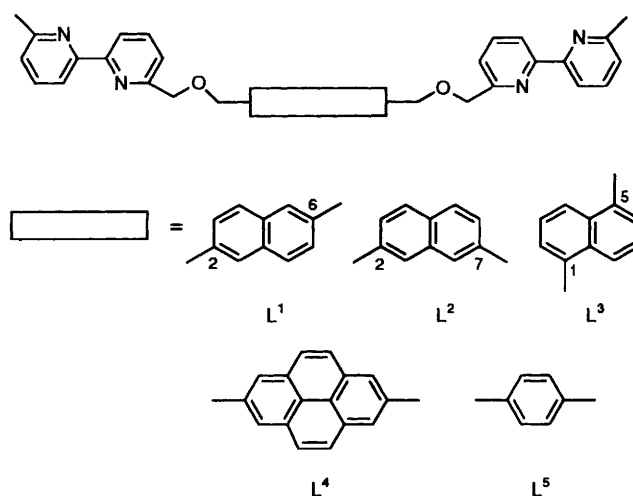
Alexander Bilyk, Margaret M. Harding,* Peter Turner and Trevor W. Hambley

School of Chemistry, University of Sydney, NSW 2006, Australia

The crystal structure of bis{2,6-bis[3-(6'-methyl-2,2'-bipyridin-6-yl)-2-oxapropyl]naphthalene}dickel tetrakis(hexafluorophosphate) $[\text{Ni}_2\text{L}^1_2][\text{PF}_6]_4$ was determined by X-ray diffraction methods and refined to a residual of 0.078 for 2765 independent observed reflections: triclinic, space group $P\bar{1}$, $a = 13.555(3)$, $b = 17.801(5)$, $c = 10.305(7)$ Å, $\alpha = 100.22(4)$, $\beta = 99.74(3)$, $\gamma = 101.83(2)^\circ$. The two nickel(II) ions are bound to four nitrogens from two bipyridyl groups and two oxygen atoms from the ether linkers in a grossly distorted octahedral geometry. The complex has a non-helical configuration and the two naphthalene rings are parallel and offset by 4.11 Å. The torsional flexibility of the ether linkers facilitates this orientation and allows the aromatic rings to stack in the complex. In solution L^1 , which contains a 2,6-disubstituted naphthalene spacer, forms non-helical and helical $[2 + 2]$ tridentate metallomacrocycles with zinc(II) (7:3) and cadmium(II) (45:55), and forms a labile complex(es) with mercury(II). No complexation with iron(II) or ruthenium(II) was observed. The effect of the substitution pattern of the naphthalene spacer was examined by comparison of the zinc(II) complexes obtained with L^1 , a 2,7-disubstituted naphthalene (L^2) and a 1,5-disubstituted naphthalene (L^3). While L^1 and L^2 both formed mixtures of $[2 + 2]$ complexes, L^3 formed a $[1 + 1]$ complex. Ligands L^1 and L^5 (containing a $p\text{-CH}_2\text{C}_6\text{H}_4\text{CH}_2$ spacer) exhibited poor ligand self-self recognition properties when treated with zinc(II).

The use of metal ions as building blocks that impart defined stereochemical and structural features on the assembly of supramolecular structures has received increasing attention in recent years.^{1,2} Due to the chirality associated with transition-metal complexes, both chiral and achiral complexes can be prepared and need to be considered in the design of supramolecular assemblies. However, the stereochemical outcome of the metal-ion assembly process can be controlled by ligand design, by matching the stereochemical preference of the metal ion with the preferred binding sites in the ligand. This approach has been clearly illustrated in the exclusive and spontaneous assembly of chiral double- and triple-helical complexes.^{3,5}

Our interest in this area has been the assembly of metallomacrocycles of defined shape and structure from two ligand molecules and two metal ions. To this end, we reported the assembly of $[2 + 2]$ bimetallic macrocycles from bis(bipyridyl) ligands L^1 , L^4 and L^5 and the metal ions Cu^I , Ag^I and Zn^{II} .^{6,7} Metal complexation may result in the formation of chiral, helical or achiral, non-helical $[2 + 2]$ complexes. The structure and number of complexes formed was found to be dependent on both the co-ordinating metal ion and the structure of the aromatic spacer. While copper(I) formed equal amounts of both chiral and achiral, labile $[2 + 2]$ tetrahedral complexes with all ligands,⁶ zinc(II) formed more stable octahedral $[2 + 2]$ complexes. Ligand L^4 formed exclusively the non-helical complex with zinc(II), which was characterized in solution and the solid state.⁷ In contrast, mixtures of helical and non-helical complexes of different stabilities were obtained with L^1 and L^5 and zinc(II), and these results were attributed to steric effects.⁷ In order further to understand the factors that determine the relative stabilities of helical and non-helical metallomacrocycles, we now report further studies of L^1 and metal ions favouring tridentate co-ordination, and include the crystal structure of the nickel(II) complex $[\text{Ni}_2\text{L}^1_2][\text{PF}_6]_4$ 1.



The effect of the position of substitution of the naphthalene ring on the metal ion assembly process, and ligand recognition studies between L^1 and L^5 and zinc(II) are also reported.

Results and Discussion

Structure of the Nickel(II) Complex $[\text{Ni}_2\text{L}^1_2][\text{PF}_6]_4$.— Treatment of an acetonitrile solution of L^1 with an equimolar amount of nickel(II) acetate afforded a pale green solution. Addition of sodium hexafluorophosphate precipitated the corresponding hexafluorophosphate salt which on recrystallisation from diethyl ether–chloroform afforded colourless crystals of $[\text{Ni}_2\text{L}^1_2][\text{PF}_6]_4$ 1. Fig. 1 shows two ORTEP views of the structure. Positional parameters are summarized in Table 1 and the nickel(II) bond lengths and angles are summarized in Table 2. The complex has the non-helical configuration and is centred around an inversion site in the triclinic space group $P\bar{1}$. Each nickel has a grossly distorted octahedral geometry (Fig.

† Supplementary data available: see Instructions for Authors, *J. Chem. Soc., Dalton Trans.*, 1995, Issue 1, pp. xxv–xxx.

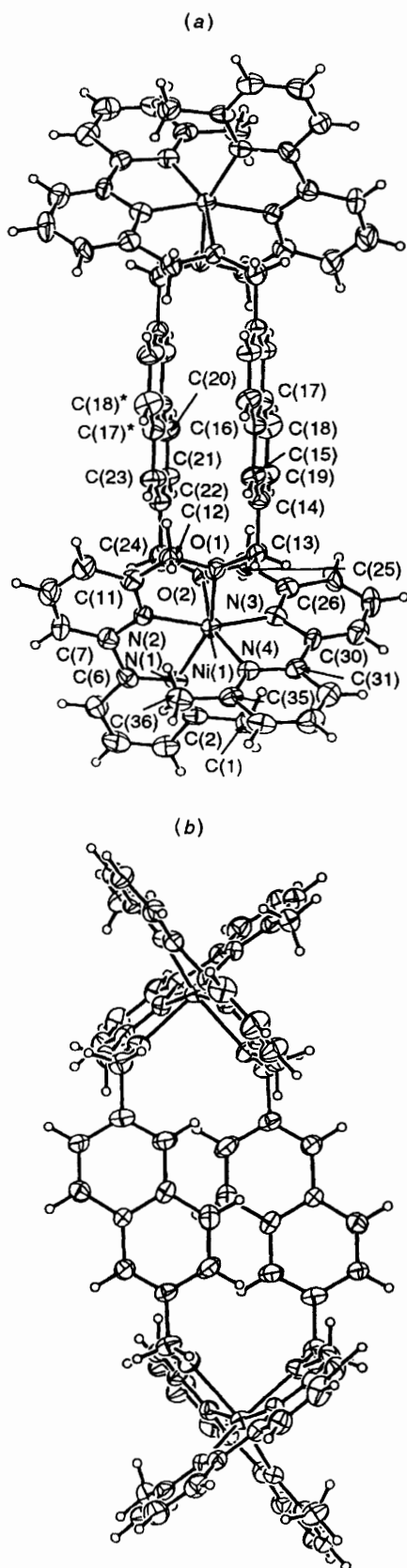


Fig. 1 ORTEP depictions of the cation $[\text{Ni}_2\text{L}^1_2]^{4+}$ (a) showing the numbering scheme; inversion related atoms are indicated with an asterisk; (b) view showing offset orientation of naphthalene rings; thermal ellipsoids are drawn at the 25% level

2), co-ordinated to two bipyridyls and two oxygens from the 2-oxapropyl linkers. The relative lateral offset of the naphthalene

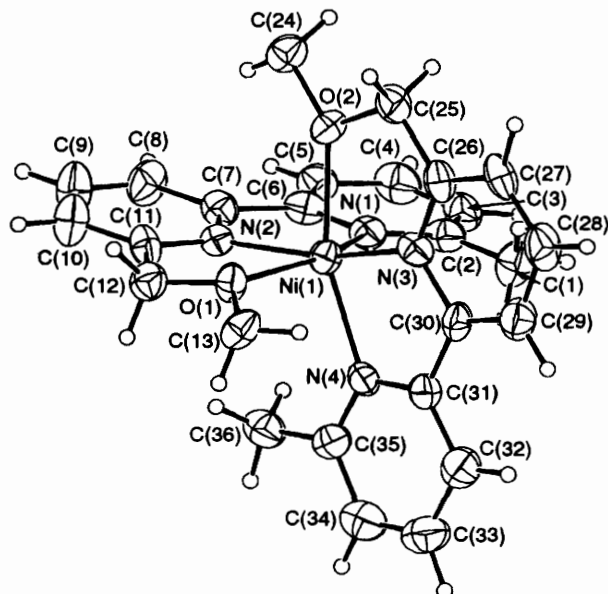


Fig. 2 The nickel co-ordination geometry in complex 1

spacers, which are separated by 3.52 Å, is 4.11 Å and the Ni...Ni distance is 12.02 Å. The complex is isomorphous with the solid-state structure of the non-helical zinc(II) complex formed by L^4 , $[\text{Zn}_2\text{L}^4_2][\text{CF}_3\text{SO}_3]_4$ **2**, which contains a pyrene spacer.⁷ For comparison, the aryl planes in **2** are separated by 3.65 Å, the lateral offset is 3.84 Å, and the Zn...Zn distance is 14.42 Å.

Six-co-ordinate nickel complexes generally exhibit regular octahedral co-ordination spheres⁸ although there are examples of distorted structures.⁹ The 89.0° dihedral angle formed by the least-squares planes of the bipyridyl residues of the nickel complex is significantly larger than the 84.6° angle found in the zinc complex **2**. The O(1)–Ni–O(2) angle is 91.1(2)°, whereas the O(1)–Zn–O(2) angle is 85.9(5)°. The co-ordination restrictions imposed by the ligand are evident in the bipyridyl plane dihedral angle of nearly 90° and the larger lateral offset of the naphthalene rings in the nickel(II) complex **1** compared to the pyrene rings in the zinc(II) complex **2**. This may be due to crystal-field stabilization energy minimization of the distorted octahedral co-ordination sphere which occurs as a result of the restricted tridentate ligand system. All of the N–Ni–N angles deviate significantly from regular octahedral values. A further indication of the co-ordination restrictions imposed by the ligand system can be found in the inequivalence of the bond angles centred on a co-ordinating atom (Table 2). The asymmetry is clearly illustrated by the Ni–O(1)–C(12) bond angle of 113.8(6)° which is considerably smaller than the Ni–O(1)–C(13) angle of 128.3(6)°.

Due to the paramagnetic nature of complex **1**, only broad NMR spectra were obtained and signal assignment was not possible. While the non-helical complex crystallized from solution, the presence of some helical complex in solution cannot be ruled out. It is interesting that in the corresponding zinc(II) complex $[\text{Zn}_2\text{L}^1_2][\text{CF}_3\text{SO}_3]_4$ **3**, all attempts to obtain crystalline material failed. In solution, the major complex **3a** was assigned to have the helical configuration on the basis of variable-temperature studies.⁷ As the zinc(II) complex **3** and the nickel(II) complex **1** are isomorphous, crystallization of the non-helical nickel(II) complex **1** may be due to an increased proportion of this complex in solution compared to the corresponding zinc(II) complex **3**, or simple fractional crystallization may have resolved the non-helical isomer. Alternatively, the contribution of stacking interactions¹⁰ to the relative stability of the non-helical complexes formed by L^1 may be more important than previously estimated,⁷ and the non-

Table 1 Positional parameters for $[\text{Ni}_2\text{L}^1_2][\text{PF}_6]_4 \mathbf{1}^*$

Atom	x	y	z	Atom	x	y	z
Ni(1)	0.2797(1)	0.1892(1)	0.1268(2)	C(10)	0.126(1)	0.3723(7)	0.122(1)
P(1)	0.4883(3)	-0.1639(2)	0.2759(4)	C(11)	0.1761(8)	0.3164(7)	0.165(1)
P(2)	0.0814(3)	-0.2138(3)	0.5718(4)	C(12)	0.2124(8)	0.3178(6)	0.305(1)
F(1)	0.4941(6)	-0.2031(4)	0.4020(7)	C(13)	0.3088(8)	0.2570(6)	0.455(1)
F(2)	0.5868(6)	-0.1921(5)	0.248(1)	C(14)	0.3705(8)	0.3333(6)	0.549(1)
F(3)	0.3912(5)	-0.1363(5)	0.3109(9)	C(15)	0.3353(8)	0.3705(6)	0.648(1)
F(4)	0.4823(8)	-0.1246(6)	0.1515(8)	C(16)	0.3955(7)	0.4439(6)	0.737(1)
F(5)	0.5608(5)	-0.0839(4)	0.3676(8)	C(17)	0.4928(8)	0.4760(6)	0.714(1)
F(6)	0.4167(5)	-0.2439(4)	0.1829(7)	C(18)	0.5283(9)	0.4365(8)	0.608(1)
F(7)	0.1583(7)	-0.2640(6)	0.5795(9)	C(19)	0.467(1)	0.3654(7)	0.526(1)
F(8)	0.121(1)	-0.1802(8)	0.463(1)	C(20)	0.6391(8)	0.5152(7)	0.159(1)
F(9)	0.0343(7)	-0.2535(7)	0.681(1)	C(21)	0.5839(8)	0.4464(6)	0.082(1)
F(10)	0.0054(8)	-0.1645(7)	0.572(1)	C(22)	0.4865(8)	0.4138(6)	0.105(1)
F(11)	0.006(1)	-0.2761(8)	0.461(1)	C(23)	0.4477(9)	0.4515(6)	0.203(1)
F(12)	0.1546(7)	-0.1528(6)	0.697(1)	C(24)	0.4236(8)	0.3345(7)	0.017(1)
O(1)	0.2810(5)	0.2682(4)	0.3181(7)	C(25)	0.5107(7)	0.2570(7)	0.137(1)
O(2)	0.4129(5)	0.2727(4)	0.0948(6)	C(26)	0.4964(8)	0.1886(6)	0.208(1)
O(3)*	0.179(3)	-0.387(2)	0.245(3)	C(27)	0.5799(7)	0.1660(7)	0.268(1)
O(4)*	0.200(2)	-0.217(2)	-0.012(2)	C(28)	0.564(1)	0.1026(8)	0.330(1)
N(1)	0.2292(6)	0.1388(5)	-0.0802(8)	C(29)	0.461(1)	0.0663(7)	0.325(1)
N(2)	0.1885(5)	0.2576(5)	0.0740(8)	C(30)	0.3812(8)	0.0908(6)	0.268(1)
N(3)	0.3985(6)	0.1546(5)	0.2059(8)	C(31)	0.2733(8)	0.0600(6)	0.260(1)
N(4)	0.2064(6)	0.0937(5)	0.1952(8)	C(32)	0.243(1)	-0.0048(7)	0.316(1)
N(5)*	0.193(2)	-0.499(1)	0.462(3)	C(33)	0.139(1)	-0.0307(8)	0.310(1)
C(1)	0.303(1)	0.0255(7)	-0.083(1)	C(34)	0.0699(9)	0.0037(8)	0.240(1)
C(2)	0.2455(8)	0.0738(6)	-0.154(1)	C(35)	0.1061(9)	0.0673(6)	0.185(1)
C(3)	0.2121(8)	0.0525(7)	-0.292(1)	C(36)	0.0321(8)	0.1039(7)	0.115(1)
C(4)	0.159(1)	0.0989(8)	-0.360(1)	C(37)*	0.115(2)	-0.460(2)	0.673(4)
C(5)	0.1380(8)	0.1636(7)	-0.286(1)	C(38)*	0.170(3)	-0.477(2)	0.558(4)
C(6)	0.1746(7)	0.1819(7)	-0.147(1)	C(39)*	0.188(2)	-0.418(2)	0.093(3)
C(7)	0.1549(7)	0.2515(7)	-0.061(1)	C(40)*	0.247(2)	-0.331(2)	0.325(3)
C(8)	0.1042(9)	0.3055(7)	-0.107(1)	C(41)*	0.195(3)	-0.295(2)	-0.057(4)
C(9)	0.092(1)	0.3650(8)	-0.014(1)	C(42)*	0.123(2)	-0.200(2)	0.063(3)

* Occupancy = 0.5.

Table 2 Nickel bond lengths (Å) and angles (°) in $[\text{Ni}_2\text{L}^1_2][\text{PF}_6]_4 \mathbf{1}$

Ni(1)–O(1)	2.205(7)	Ni(1)–N(2)	1.984(8)
Ni(1)–O(2)	2.202(6)	Ni(1)–N(3)	1.943(8)
Ni(1)–N(1)	2.098(8)	Ni(1)–N(4)	2.084(8)
O(1)–Ni(1)–O(2)	91.1(2)	N(3)–Ni(1)–N(4)	79.7(3)
O(1)–Ni(1)–N(1)	155.2(3)	Ni(1)–O(1)–C(12)	113.8(6)
O(1)–Ni(1)–N(2)	75.5(3)	Ni(1)–O(1)–C(13)	128.3(6)
O(1)–Ni(1)–N(3)	92.9(3)	Ni(1)–O(2)–C(24)	133.8(6)
O(1)–Ni(1)–N(4)	89.7(3)	Ni(1)–O(2)–C(25)	115.3(6)
O(2)–Ni(1)–N(1)	92.5(3)	Ni(1)–N(1)–C(2)	130.1(8)
O(2)–Ni(1)–N(2)	90.0(3)	Ni(1)–N(1)–C(6)	112.5(7)
O(2)–Ni(1)–N(3)	75.8(3)	C(2)–N(1)–C(6)	117.3(9)
O(2)–Ni(1)–N(4)	155.5(3)	Ni(1)–N(2)–C(7)	117.0(7)
N(1)–Ni(1)–N(2)	80.0(3)	Ni(1)–N(2)–C(11)	121.0(7)
N(1)–Ni(1)–N(3)	111.7(3)	Ni(1)–N(3)–C(26)	124.6(8)
N(1)–Ni(1)–N(4)	96.9(3)	Ni(1)–N(3)–C(30)	118.2(6)
N(2)–Ni(1)–N(3)	161.7(3)	Ni(1)–N(4)–C(31)	112.4(6)
N(2)–Ni(1)–N(4)	113.8(3)	Ni(1)–N(4)–C(35)	127.5(8)

helical complex may be the predominant species present in both **1** and **3**.

Studies with other Metal Ions.—Attempts to complex L^1 with cadmium, mercury, iron and ruthenium were made in order to establish the effect of the metal ions on the outcome of the assembly process. In solution, the cadmium(II) complex formed two complexes in the ratio 2:3 suggesting that both helical and non-helical tridentate labile [2 + 2] complexes were present in solution. A mercury(II) complex was isolated but the NMR spectrum of this product was extremely broad, suggesting a

labile complex undergoing exchange on the NMR time-scale. Attempts to prepare iron(II) and ruthenium(II) complexes were unsuccessful probably due to the severely distorted octahedral geometry required by the tridentate ligand L^1 which is not readily accommodated by these two metals.

Recognition Studies.—A ligand self-recognition experiment was carried out between the readily available ligands L^1 and L^5 with zinc(II) in order to see whether [2 + 2]metallo-macrocycles formed by the same two ligand strands were observed. Such recognition has been reported in the case of the copper(I) helicates which assemble with positive cooperativity, the binding of one copper(I) with two ligands facilitating the complexation of the next one.³ Similarly, in the case of palladium(II) molecular boxes, initial kinetic products are formed but after prolonged heating the thermodynamic box-product was cleanly and exclusively formed in the reaction mixture.¹¹

Equimolar amounts of the L^1 and L^5 in acetonitrile were treated with 2 equivalents of zinc(II). The crude product was isolated and analysed by NMR spectroscopy without purification. Analysis of the aromatic region of the spectrum ($\delta \approx 6.0\text{--}7.5$) showed the aromatic signals that are characteristic of the metallomacrocycles, but in addition to the signals previously assigned to the complexes $[\text{Zn}_2\text{L}^1_2][\text{CF}_3\text{SO}_3]_4$ and $[\text{Zn}_2\text{L}^5_2][\text{CF}_3\text{SO}_3]_4$, other minor resonances were observed, consistent with formation of the helical and non-helical mixed-ligand complexes $[\text{Zn}_2\text{L}^1\text{L}^5][\text{CF}_3\text{SO}_3]_4$ (Fig. 3). However, a simple statistical mixture of complexes was not observed and the major complexes were indeed the [2 + 2]metallo-macrocycles formed from the same ligand strands. Thus, while some ligand self-recognition was achieved, multiple complexes formed, undoubtedly as a result of the relatively long linkers

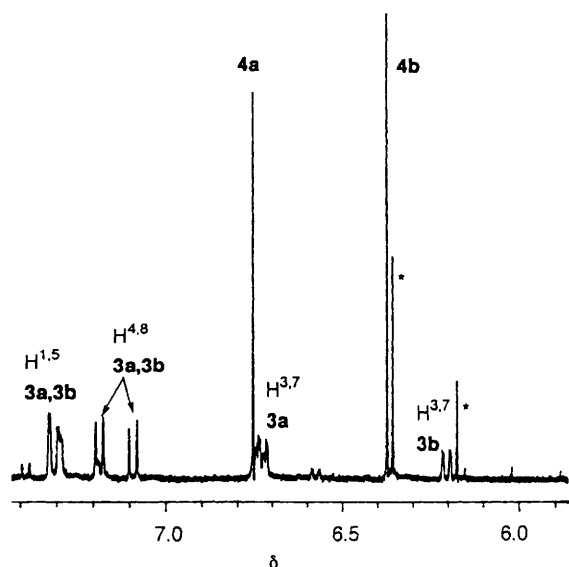


Fig. 3 Portion of 400 MHz ¹H NMR spectrum of product obtained on treatment of L¹ and L⁵ with zinc(II) to give predominantly [Zn₂L₂][CF₃SO₃]₄ 3 and [Zn₂L₅][CF₃SO₃]₄ 4; starred peaks are due to phenyl resonances from mixed-ligand complexes containing L⁵

and aromatic spacers that separate the co-ordination sites in the ligands.

Effect of Naphthalene Substitution Pattern.—The crystal structures of 1 and the isomorphous zinc(II) complex [Zn₂L⁴][CF₃SO₃]₄ 2 reinforce the importance of the balance between flexibility and rigidity of the 2-oxapropyl linkers in the ligand design. As zinc(II) forms diamagnetic bipyridyl complexes, which are readily characterised in solution by NMR spectroscopy, the effect of the naphthalene substitution pattern on the outcome of the assembly process was examined by comparison of the complexes obtained with L¹, L² and L³ and zinc(II). Previously, we reported that L¹ gives a mixture of complexes in the ratio 70:30. Ligand L², which contains a 2,7-disubstituted naphthalene linker, assembled into a mixture of helical and non-helical complexes in the ratio 45:55. Absolute assignment of configuration was not possible, but clearly the energy difference between the complexes is very small. In contrast, the zinc(II) complex formed from L³, the 1,5-disubstituted naphthalene ligand, exhibited only broad signals in the NMR spectrum at room temperature. At low temperature, these signals sharpened, and on the basis of upfield chemical shift data, the complex was tentatively assigned as a 1:1 complex in which two bipyridyl groups from the same ligand molecule are directed under the naphthalene ring to complex a single zinc(II) atom.

Thus, both the 2,6- and 2,7-disubstituted naphthalene bis(bipyridyls) assemble into mixtures of helical and non-helical metallomacrocycles. In energetic terms, the differences in stabilities of the complexes are small. The 1,5-naphthalene substitution pattern of ligand L³ does not favour formation of metallomacrocycles and results in a mixture of products.

Experimental

Melting points were determined on a Reichert heating stage and are uncorrected. Ultraviolet spectra were recorded on a Hitachi 150-20 spectrophotometer. NMR spectra were recorded on a Bruker AMX400 spectrometer. Spectra were recorded in the solvent indicated, locked on solvent deuterium and referenced to residual solvent protons. Electrospray (ES) mass spectra were recorded at the University of Wollongong on a Vestec

model M-200 electrospray mass spectrometer. Samples were introduced in MeCN–water at 3–5 μl min⁻¹.

Synthesis of L² and L³.—Ligands L² and L³ were prepared by the same general method⁶ used for the preparation of L¹.

2,7-Bis[3-(6'-methyl-2,2'-bipyridin-6-yl)-2-oxapropyl]naphthalene (L²) was obtained as off-white crystals (280 mg, 49%): m.p. 145 °C (Found: C, 78.5; H, 6.0; N, 9.9. Calc. for C₃₆H₃₂N₄O₂: C, 78.2; H, 5.8; N, 10.1%). ¹H NMR (400 MHz, CDCl₃): δ 2.67 (s, CH₃), 4.83, 4.87 (2s, CH₂), 7.18 (d, *J* 7.6, H^{3''}), 7.55 (dd, *J* 8.2, 1.6, H^{3,6}), 7.56 (d, *J* 7.5, H⁵), 7.71 (dd, *J* 7.7, H^{4''}), 7.83–7.87 (m, H^{1,4,5,8,4'}), 7.21 (d, *J* 7.8, H^{3'}) and 8.47 (d, *J* 7.8 Hz, H^{3''}). ES mass spectrum: *m/z* 553 [*M* + H⁺], 277.2 [*M* + H₂²⁺], 195.0, 177.2, 171.1, 98.0.

1,5-Bis[3-(6'-methyl-2,2'-bipyridin-6-yl)-2-oxapropyl]naphthalene (L³) was recrystallised from ethyl acetate to give white plates (340 mg, 62%): m.p. 171–172 °C (Found: C, 78.0; H, 6.0; N, 10.0. Calc. for C₃₆H₃₂N₄O₂: C, 78.2; H, 5.8; N, 10.1%). ¹H NMR (400 MHz, CDCl₃): δ 2.65 (s, CH₃), 4.85, 5.16 (2s, CH₂), 7.17 (d, *J* 7.6, H^{3''}), 7.50 (d, *J* 7.5, H⁵), 7.52 (dd, *J* 8.4, 6.9, H^{3,7}), 7.61 (d, *J* 6.9, H^{2,6}), 7.70 (dd, *J* 7.7, H^{4''}), 7.81 (dd, *J* 7.7, H⁴), 8.21 (d, *J* 7.8, H^{3,4,8}) and 8.47 (d, *J* 7.8 Hz, H^{3''}). ES mass spectrum: *m/z* 553 [*M* + H⁺], 277.2 [*M* + H₂²⁺], 184.1, 177.2, 155.2, 98.0.

Reactions of L¹.—*With nickel(II).* Nickel acetate tetrahydrate (13 mg, 53 μmol) and L¹ (30 mg, 54 μmol) were added to methanol (20 cm³) and heated at reflux for 1 h. The mixture was cooled, filtered and ammonium hexafluorophosphate (200 mg, 1.2 mmol) in methanol (5 cm³) was added. The precipitate was collected and washed with copious amounts of water, chloroform and diethyl ether to give [Ni₂L¹][PF₆]₄ 1 as a pale blue powder which was dried under high vacuum for 24 h (39 mg, 82%) (Found: C, 48.0; H, 3.9; N, 5.9. Calc. for C₇₆H₆₄F₂₄N₈Ni₂O₄P₄: C, 48.0; H, 3.6; N, 6.2%). λ_{max} MeCN (log ε/dm³ mol⁻¹ cm⁻¹): 202 (5.05), 228 (5.23), 246 (4.63), 292 (4.69), 300 (4.67) and 312 nm (4.59). ES mass spectrum: *m/z* 1657 [(*M* – PF₆)³⁺], 756.6 [(*M* – 2 PF₆)²⁺].

With Cd(CF₃SO₃)₂. Cadmium acetate (15.5 mg, 67 μmol) and L¹ (37.4 mg, 68 μmol) were added to methanol (10 cm³) and the mixture was heated at reflux for 2 h. The reaction mixture was cooled, filtered and ammonium hexafluorophosphate (200 mg, 810 μmol) in methanol (5 cm³) was added. The resultant precipitate was collected and washed with methanol to give [Cd₂L¹][PF₆]₄·H₂O as a white powder (41 mg, 64%) (Found: C, 44.2; H, 3.7; N, 5.6. Calc. for C₇₂H₆₄Cd₂F₂₄N₈O₄P₄: C, 44.4; H, 3.5; N, 5.8%). ¹H NMR (400 MHz, CD₃CN): δ 2.83, 2.32 (s, CH₃), 4.08 and 4.37 (AX system, *J* 13.2, CH₂), 4.04 and 4.47 (AX system, *J* 14.0, CH₂), 4.70 and 4.91 (AX system, *J* 16.0, CH₂), 4.87 and 4.97 (AX system, *J* 16.4, CH₂), 6.84 (d, *J* 8.4, H^{3,7}), 6.93 (d, *J* 8.4, H^{3,7}), 7.10 (d, *J* 8.4, H^{4,8}), 7.21 (d, *J* 8.4, H^{4,8}), 7.30 (br s, H^{1,5}), 7.42 (br s, H^{1,5}), 7.56 (br d, *J* 8.4 Hz), 7.68–7.77 (m), 8.23–8.39 (m) and 8.49–8.66 (m). λ_{max}(MeCN) (log ε/dm³ mol⁻¹ cm⁻¹): 202 (5.02), 230 (5.27), 244 (4.66), 292 (4.72), 300 (4.70) and 314 nm (4.57).

Reactions of L².—*With zinc(II).* Using the method previously reported,⁷ L² (42 mg, 76 μmol) was treated with Zn(O₃SCF₃)₂ to give the complex [Zn₂L²][CF₃SO₃]₄·2H₂O as a light yellow solid (55 mg, 79%) (Found: C, 48.8; H, 3.9; N, 5.9. Calc. for C₇₆H₆₈F₁₂N₈O₁₈S₄Zn: C, 48.8; H, 3.9; N, 5.9%). ¹H NMR (400 MHz, CD₃CN): δ 1.98, 1.99 (2s, CH₃), 3.58 and 4.27 (AX system, *J* 13.4, CH₂), 3.76 and 4.30 (AB system, *J* 13.2, CH₂), 4.72 and 4.76 (AB system, *J* 15.9, CH₂), 4.87 and 4.95 (AB system, *J* 15.7, CH₂), 6.42, 6.74 (2dd, *J* 1.6 and 8.4, H^{3,6}), 6.91, 7.09 (2br s, H^{1,8}), 7.43, 7.45 (d, *J* 8.4, H^{4,5}), 7.62 (d, *J* 8.1, H^{5''}), 7.69 (d, *J* 8.1, H⁵), 8.27–8.36 (m, H^{4,4''}), 8.56, 8.57 (2d, *J* 8.0, H^{3'}) and 8.61, 8.63 (d, *J* 7.9 Hz, H³). λ_{max}(MeCN) (log ε/dm³ mol⁻¹ cm⁻¹): 202 (4.99), 230 (5.28), 244 (4.63), 292 (4.70), 300 (4.69) and 316 nm (4.59). ES mass spectrum: *m/z* 767 [(*M* – 2 CF₃SO₃)²⁺], 553 [L² + H⁺], 461.5 [(*M* – 3

CF_3SO_3^+], 309 $[(M - 4 \text{CF}_3\text{SO}_3)]$ and 277 $[(L^2 + 2H)^{2+}]$.

X-Ray Crystallography.—Diffraction quality crystals were grown by slowly infusing diethyl ether into an acetonitrile solution of complex 1. The crystals decompose within seconds of being removed from the precipitant. Accordingly, a colourless oblong crystal of dimensions $0.95 \times 0.1 \times 0.075$ mm was injected with diethyl ether into a thin walled glass capillary. Sufficient diethyl ether was removed to expose the crystal and the capillary was then sealed.

Lattice parameters at 21 °C were determined by least-squares fit to the setting parameters of 25 independent reflections, measured and refined on a direct drive Rigaku AFC7R four-circle diffractometer employing graphite-monochromated Cu-K α radiation. Intensity data were collected in the range $4 < \theta < 120^\circ$ using an ω - 2θ scan, with a scan width of $(1.21 + 0.35 \tan \theta)^\circ$. Three standard reflections measured every 150 reflections showed no significant change during the data collection. Data reduction and application of Lorentz, polarization and psi-scan absorption corrections were carried out using the TEXSAN structure determination software package.¹² The structure was solved by direct methods using SHELXS 86¹³ and the solution was extended by difference Fourier methods using the TEXSAN program suite. Scattering factors and anomalous dispersion terms used were those incorporated in the TEXSAN package.¹³ Non-hydrogen atoms of the complex were refined anisotropically with full-matrix least squares. Hydrogen atoms were included at calculated sites with group isotropic thermal parameters. Two acetonitrile solvate molecules and the C–O–C core of a diethyl ether molecule were included in the refined model with occupancies of 0.5. The diethyl ether methyl sites could not be located. Hydrogen atoms were attached to one of the acetonitrile molecules; the carbon and nitrogen atoms of the second acetonitrile molecule could not be distinguished. The atom numbering scheme is given in Fig. 1. Plots were drawn using ORTEP.¹⁴

Crystal data. $\text{C}_{78}\text{H}_{67}\text{F}_{24}\text{N}_9\text{Ni}_2\text{O}_6\text{P}_4$, $M = 1923.70$, triclinic, space group $P\bar{1}$, $a = 13.555(3)$, $b = 17.801(5)$, $c = 10.305(7)$ Å, $\alpha = 100.22(4)$, $\beta = 99.74(3)$, $\gamma = 101.83(2)^\circ$, $U = 2340(2)$ Å³, $D_c(Z = 1) = 1.365$ g cm⁻³, $\mu(\text{Cu-K}\alpha) = 20.28$ cm⁻¹, $\lambda(\text{Cu-K}\alpha) = 1.5418$ Å, $F(000) = 978$ electrons. Ranges of hkl 0–15, –20 to 20, –12 to 12, N (total) = 7329, N (unique) = 6983 ($R_{\text{merge}} = 0.04$), $N_o = 2765$ [$I > 2.0\sigma(I)$], $N_{\text{var}} = 576$, $R = 0.078$, $R' = 0.080$, residual extrema –0.34 to 0.44 e Å⁻³.

Additional material available from the Cambridge Crystallographic Data Centre comprises H-atom coordinates, thermal parameters and remaining bond lengths and angles.

Acknowledgements

Financial support from the Australian Research Council and partial support from the Cooperative Research Centre

for Molecular Engineering and Technology is gratefully acknowledged.

References

- 1 E. C. Constable, *Chem. Ind. (London)*, 1994, 56 and refs. therein; *Nature (London)*, 1990, **346**, 314; 1993, **362**, 412 and refs. therein.
- 2 *Perspectives in Coordination Chemistry*, eds. A. F. Williams, C. Floriani and A. E. Merbach, VCH, Weinheim, 1992.
- 3 J.-M. Lehn, A. Rigault, J. Siegel, J. Harrowfield, B. Chevrier and D. Moras, *Proc. Natl. Acad. Sci. USA*, 1987, **84**, 2565; J.-M. Lehn and A. Rigault, *Angew. Chem., Int. Ed. Engl.*, 1988, **27**, 1095; U. Koert, M. M. Harding and J.-M. Lehn, *Nature (London)*, 1990, **346**, 339; T. M. Garrett, U. Koert, J.-M. Lehn, A. Rigault, D. Meyer and J. Fisher, *J. Chem. Soc., Chem. Commun.*, 1990, 557; R. Krämer, J.-M. Lehn, A. De Cian and J. Fisher, *Angew. Chem., Int. Ed. Engl.*, 1993, **32**, 703.
- 4 E. C. Constable and M. D. Ward, *J. Am. Chem. Soc.*, 1990, **112**, 1256; E. C. Constable, *Angew. Chem., Int. Ed. Engl.*, 1991, **30**, 1450; E. C. Constable, S. M. Elder, J. Healy and M. D. Ward, *J. Am. Chem. Soc.*, 1990, **112**, 4590; E. C. Constable, M. J. Hannon and D. A. Tocher, *J. Chem. Soc., Dalton Trans.*, 1993, 1883.
- 5 A. F. Williams, C. Piguat and G. Bernardinelli, *Angew. Chem., Int. Ed. Engl.*, 1991, **11**, 1490; C. Piguat, G. Bernardinelli and A. F. Williams, *Inorg. Chem.*, 1989, **28**, 2920; C. Piguat, G. Bernardinelli, B. Bocquet, A. Quattropane and A. F. Williams, *J. Am. Chem. Soc.*, 1992, **114**, 7440; S. Rüttiman, C. Piguat, G. Bernardinelli, B. Bocquet and A. F. Williams, *J. Am. Chem. Soc.*, 1992, **114**, 4230.
- 6 A. Bilyk and M. M. Harding, *J. Chem. Soc., Dalton Trans.*, 1994, 77.
- 7 A. Bilyk, M. M. Harding, P. Turner and T. W. Hambley, *J. Chem. Soc., Dalton Trans.*, 1994, 2783.
- 8 L. Sacconi, F. Mani and A. Bencini, in *Comprehensive Coordination Chemistry*, ed. G. Wilkinson, Pergamon, 1987, vol. 5, ch. 50, p. 1; B. J. Hathaway, in *Comprehensive Coordination Chemistry*, ed. G. Wilkinson, Pergamon, 1987, vol. 5, ch. 53, p. 533.
- 9 A. Clausen and A. C. Hazell, *Acta Chem. Scand.*, 1970, **24**, 2811; E. Larsen, G. N. La Mar, B. E. Wagner, J. E. Parks and R. H. Holm, *Inorg. Chem.*, 1972, **11**, 2652.
- 10 C. A. Hunter and J. K. M. Sanders, *J. Am. Chem. Soc.*, 1990, **112**, 5525.
- 11 M. Fujita, J. Yazaki and K. Ogura, *J. Am. Chem. Soc.*, 1990, **112**, 5645; *Chem. Lett.*, 1991, 1031; *Tetrahedron Lett.*, 1991, 5589.
- 12 TEXSAN, Single Crystal Structure Analysis Software, Version 1.6, Molecular Structure Corporation, The Woodlands, Houston, TX, 1993.
- 13 SHELXS 86, G. M. Sheldrick, in *Crystallographic Computing 3*, eds. G. M. Sheldrick, C. Krüger and R. Goddard, Oxford University Press, 1985, pp. 175–188.
- 14 C. K. Johnson, ORTEP-II, A FORTRAN Thermal Ellipsoid Plotting Program, Report ORNL-5138, Oak Ridge National Laboratories, Oak Ridge, TN, 1976.

Received 14th March 1995; Paper 5/01600B